# SIFT AND GABOR FEATURES FOR VERY HIGH RESOLUTION IMAGE CLASSIFICATION

*Chahrazed FIALA, Abdelhamid DAAMOUCHE*

Signals and Systems Laboratory, Institute of Electrical and Electronic Engineering, University M'hamed Bougara, Boumerdes

***Abstract*—this paper presents a new approach to extract features from high resolution images inspired by the sift descriptor and gabor features. both of these two methods are powerful when used separately or together in region-based or pixel-based classification, they brought a high accuracy. our approach was applied to classify two very high resolution images of boumerdes (algeria) and djeddah (ksa) using knn and svm. the obtained results achieved promising performance compared to using spectral information alone.**

***Index Terms*—** SIFT, 2-D GABOR FILTER, VHR IMAGES, KNN, SVM.

## 1. INTRODUCTION

Several approaches and methods of processing and classification were developed and led to establishing algorithms for filtering, segmentation, extraction of features and classification of VHR image [1, 2, 3, 4, 5]. Among powerful filters used to smooth regions of this category of images, there is the Gabor filter, its application improves accuracy [6,7]. Similarly, SIFT used to extract descriptors for classification or matching patches of specific regions [8]. Good results were reported when these two powerful tools were involved [9]. This motivated us to propose a new approach for the VHR images based on SIFT and Gabor filter. Indeed, it consists of applying the Gabor filter to the image where the pixel-based method is adopted; which led us to keep only the necessary steps of SIFT to extract features, also the RGB information is added to construct features for the purpose of classification. The method is applied to Boumerdes and Djeddah images to test its robustness. For that purpose, three models of descriptors are constructed: Bag of Gradiant Features (B.G.F), Bag of Orientation Features (B.O.F), and Bag of Gradiant Features and RGB Information(B.G.F.I), then models of classification were built using KNN and SVM classifiers.

A brief review of the Gabor filter and SIFT is necessary before presenting our new approach.

## 2. GABOR FILTER

In image processing, the 2-D Gabor filter is widely used; it is characterized by spatial localization, orientation, and frequency [10]. This filter is a multiplication of complex sinusoid and Gaussian function [11], where $s(x,y)$ is the carrier and $w(x,y)$ is the envelope. That is:

- $(x_0, y_0)$: the center of the envelope.
- $K, a$ and $b$ : the scale of the magnitude and scales of the two axes of the envelope. Where $\sigma_x = 1/a$ and $\sigma_y = 1/b$.
- $f_0, w_0$ : magnitude and orientation of the spatial frequency.
- $\theta$ : rotation of the Gaussian envelope.
- $\varphi$ : phase of the carrier.

The filter equation is simplified as below.

$$g(x,y) = s(x,y).w(x,y) = [exp(j(2\pi f_0(x\cos w_0 + y\sin w_0)) + \varphi)] . [K exp(-\pi(a^2((x-x_0)\cos\theta + (y-y_0)\sin\theta) + b^2((x-x_0)\sin\theta + (y-y_0)\cos\theta))] \quad (1)$$

## 3. SIFT

The Scale Invariant Feature Transform (SIFT) is applied to extract features from the image of an object or a scene, and compare them with others even if they do not have the same orientation or illumination [12]. The SIFT is applied to region classification of a VHR image to extract descriptors from patches which are used as patterns of regions. Once correctly classified, they are used as benchmarks to construct a true map from a satellite image.

## 4. THE PROPOSED APPROACH

Our approach is based on the SIFT and the Gabor filter to extract features. It is applied to the VHR images. All the pixels of the image are treated due to the dimension of land covered by a pixel. In order to achieve our aim, which is getting the best features representing a pixel, the following steps were done. First, the RGB information matrix (RGB) is extracted from the query image, then the latter was smoothed by the real part of the complex Gabor filter (equation (1)) where $w_0 = 0,$ 1 and $k = \sqrt{ab}$. The envelope is centralized on the origin. This filter homogenizes information of the same region. Second, SIFT, without selecting keypoint steps, is applied to extract vectors of gradient and orientation for the whole image. Third, the bags of features were constructed from the gradient or orientation vectors or both of them (B.G.F or B.O.F ), and the RGB information (B.G.F.I). Fourth, for each fixed value of $\sigma$ ($\sigma_x = \sigma_y = \sigma$ ), two supervised models of classification were trained, using KNN and SVM. Fifth, the accuracy was calculated using the test set. Sixth, according to accuracy, the value of σ was adjusted, and then all the steps were repeated. Finally, the process was repeated until a high accuracy was attained. We illustrate these steps in figure 1.

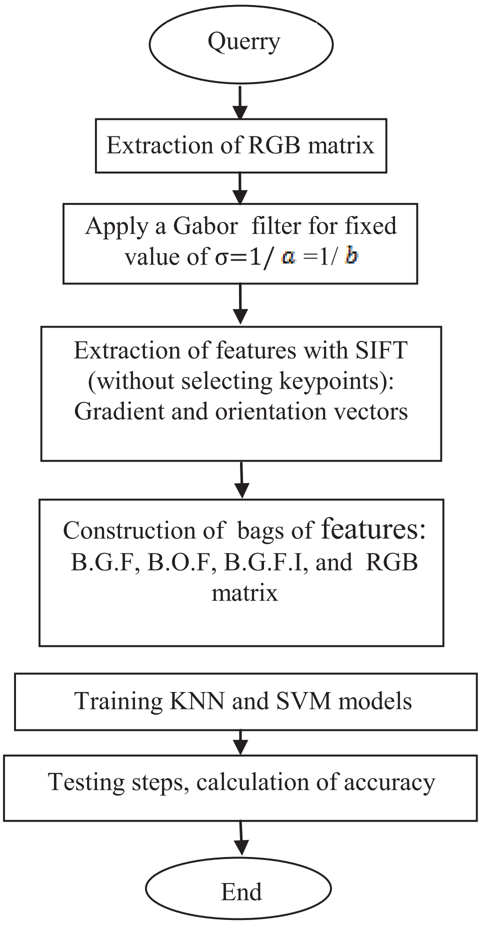


Figure 1: Workflow of feature extraction based on Gabor filter, SIFT, and RGB information.

## 5. APPLICATION OF THE PROPOSED APPROACH TO BOUMERDES AND JEDDAH IMAGES

Our approach was applied to Boumerdes and Djedda images (see fig.2 and fig. 3).

Figure 2: “Rocher noir” on the coast of Boumerdes, Algeria.

Figure 3: A region on Djeddah coast, ASK

### 5.1. TRAINING AND TEST SETS CONSTRUCTION

The features were constructed as described in Section 6. Then, several regions representing the ground truth are chosen to form the training and test sets. Eleven (11) classes were selected from the image of Boumerdes (sea, dry sand, wet sand, rocks, roof1, roof2, asphalt, grass, tree, pavement, and bare soil). First, the KNN classifier is used to assess the performance of the descriptors using a training set of 37 patches (1813pixels), then a set of 44 patches ( 2156 pixels), finally a set of 86 patches (4214). Further, in section 7.2, the results show that the best model of a classifier is obtained for the training set of 86 patches, so the later is kept for the rest of our work. With regards to the image of Djeddah, seven (7) classes were selected (sea, roof3, asphalt, pavement, tree, and grass). The values of σ belong to [0.5, 2.6] due to the ground truth of first model diversity. Each image was treated separately. The models, using KNN and SVM, were trained. After testing the models, the process is repeated until the best accuracy is obtained. The results are given in the next section.

## 5.2. RESULTS AND DISCUSSION

We note that for several σ values, only those of B.G.F and B.G.F.I for both images were presented in tables 1 and 2 for the assessment of our approach. Where OA stands for the Overall Accuracy, AA is the Average Accuracy.

Table 1 presents the obtained accuracy using the KNN classifier for three sizes of the training set. Only the B.G.F is tested at first and the best results are given. It is noted that the higher size leads to the best accuracy. Indeed, increasing the number of patterns enhances learning and improves the class separation in our case.

Table 2 shows the obtained accuracy using the KNN classifier. It is clear that the B.F.G.I achieved the best results.

Table 3 summarizes the accuracy obtained by the SVM classifier for B.G.F, B.G.F.I and RGB. The results show that B.G.F.I achieved the highest accuracy for both images and σ =1.5.

It is noted that the best results were achieved for different values of σ for both B.G.F (σ =0.5) and B.G.F.I (σ=1.5), and for both images, this confirms that their choice remains empirical. Also, our bag of features constructed from gradients is not sufficient for discrimination, but after adding the RGB information the accuracy increased for both images.

TABLE 1: THE OBTAINED CLASSIFICATION RESULTS USING KNN FOR SEVERAL SIZES OF THE TRAINING SET

| Training set size (number of pixels) | 1813 | 2156 | 4214 |
|---|---|---|---|
| OA for B.G.F (%) | 36.89 | 53.99 | 69.64 |

TABLE 2: THE OBTAINED CLASSIFICATION RESULTS USING KNN

| | | B.G.F | | B.G.F.I | |
|---|---|---|---|---|---|
| $\sigma$ | K | Boumerdes OA % | Djeddah OA % | Boumerdes OA % | Djeddah OA % |
| 0.5 | 1 | **69.64** | 49.30 | **71.88** | 55.75 |
| | 2 | 68.98 | 49.90 | 71.67 | 55.75 |
| 1.9 | 1 | 68.70 | 49.13 | 71.29 | 79.86 |
| | 2 | 68.22 | **50.25** | 70.98 | 77.46 |
| 2.1 | 1 | 67.19 | 45.37 | 69.67 | **80.18** |
| | 2 | 66.80 | 45.49 | 69.27 | 78.11 |

TABLE 3: THE OBTAINED CLASSIFICATION RESULTS USING SVM

| | | Boumerdes Image | Djeddah Image |
|---|---|---|---|
| OA % | B.G.F | 78.12 | 85.09 |
| | B.G.F.I | **81.27** | **85.68** |
| | RGB | 78.04 | 79.41 |
| AA % | B.G.F | 75.20 | 82.06 |
| | B.F.G.I | **79.47** | **81.32** |
| | RGB | 75.18 | 75.48 |

## 8. CONCLUSION

Our approach was applied to a VHR RGB image, where all pixels are treated. Enhancing the texture of regions with Gabor filter before extracting features led to high accuracy, however, the choice of its parameters remains empirical. Several bags of features constructed from gradients, orientations and RGB information were used to train the classifiers by KNN and SVM for eleven (11) and seven (7) classes, then tested. Only the B.F.G.I achieved the best average accuracy for both images.

Our results are promising and motivate us, for the next work, to take advantage of the high dimension of our feature vectors and extending the number of classes. We aim to train models of classification using data from several images, covering land's diversity, in order to obtain high accuracy and reproduce a reliable map of the ground truth.

## REFERENCES


[1] L. Maa,b, M. Lia, X. Ma, L. Cheng, P. Du, Y. Liu, "A Review of Supervised Object-based Land-Cover Image classification," *Journal of Photogrammetry and Remote Sensing* 130*,* 277–293, 2017.

[2] A. Izadipour, Behzad Akbari, Barat Mojaradi, "A new feature selection method for segmentation of VHR satellite image," *IEEE ICCSPA'15*, April 2015.

[3] O. Regniers, L.Bombrun, V.Lafon, C. Germain, "Supervised Classification of Very High Resolution Optical Images Using Wavelet-Based Textural Features," *IEEE Transactions on Geoscience and Remote Sensing, Institute of Electrical and Electronics Engineers*, 3722-3735, 2016.

[4]Z. Y. Lv, J. Shia, Y. Wanga, "An Adaptive Morphological Mean Filter For Very High-Resolutionremote Sensing Image Processing," *The International Archives of the Photogrammetry, Remote Sensing and Spatial Information Sciences*, Volume XLII-2/W7, 2017.

[5] M. T. Pham, G. Mercier, O. Regniers, and J. Michel, "Texture Retrieval from VHR Optical Remote Sensed Images using the Local Extrema Descriptor with Application to Vineyard Parcel Detection," *Remote Sensing, MDPI*, 2016, 8 (368), pp.1 – 21, hal-01311993, 2016.

[6] L.Chen, Q. Zhu, X. Xie, H. Hu, and H. Zeng, " Road Extraction from VHR Remote-Sensing Imagery via Object Segmentation Constrained by Gabor Features," ISPRS Int. J. Geo-Inf. 7, 362, September 2018.

[7] Z. Li, W.Shi, H.Zhang, M. Hao, "Change Detection Based on Gabor Wavelet Features for Very High Resolution Remote Sensing Images," *IEEE Geoscience and Remote Sensing Letters*, Volume: 14, Issue: 5,783-787, May 2017.

[8] B.Sirmacek, C. Unsalan, " Urban-Area and Building Detection Using SIFT Keypoints and Graph Theory, " *IEEE Trans. Geosci. Remote Sens*. ,47, 1156–1167, 2009.

[9] Y. Yang and S. Newsam, "Comparing SIFT Descriptors AND Gabor Texture Features For Classification Of Remote Sensed Imagery," *IEEE, 15th IEEE International Conference on Image Processing*. 2008

[10] U. Marmol, "Use of Gabor filters for Texture Classification of Airborne Images and LIDAR," *Archives of Photogrammetry, Cartography, and Remote Sensing*, Vol. 22, pp. 325-336, 2011.

[11] J.R. Movellan, "Tutorial on Gabor Filters," http://citeseerx.ist.psu.edu/viewdoc/download?doi=10.1.1.370.3513&rep=rep1&type=pdf.

[12] D. Lowe, "Distinctive image features from scale-invariant keypoints," *IJCV,* 60(2):91–110, 2004. ISSN 2083-2214.